3. SITE 1074[1]

Shipboard Scientific Party[2]

HOLE 1074A

Position: 22°46.8326′N, 46°6.7398′W

Start hole: 1315 hr, 1 August 1997

End hole: 0520 hr, 2 August 1997

Time on hole: 16.08 hr

Seafloor (drill-pipe measurement from rig floor, mbrf): 4457.1

Total depth (drill-pipe measurement from rig floor, mbrf): 4526.6

Distance between rig floor and sea level (m): 11.6

Water depth (drill-pipe measurement from sea level, m): 4445.5

Penetration (mbsf): 69.5

Coring totals:

Type: APC; Number: 7; Cored: 63.5 m; Recovered: 65.8 m (103.6%)
Type: XCB; Number: 1; Cored: 6.0 m; Recovered: 0.58 m (9.67%)

Lithology:

Unit I (0.0–63.5 mbsf): Nannofossil ooze with foraminifers, clay, radiolarians, and sand; nannofossil clay
Unit II (63.5–69.5 mbsf): Aphyric basalt

Principal results: Sixty-four meters of sediment and 0.58 m of basalt were recovered at the single hole drilled at Site 1074. A total of eight cores were recovered; Cores 174B-1074A-1H through 7H contain sediments, and Core 8X is basalt. Two lithologic units were defined: Unit I contains nannofossil ooze with varying amounts of foraminifers, clay, radiolarians and sand, and nannofossil clay, overlying Unit II, which is a unit of aphyric basalt. The sedimentary Unit I was divided into two subunits based on the magnetic susceptibility record, clay content, and the presence or absence of graded sand layers. Subunit IA includes the upper 62 m of sediments; Subunit IB, a red clay, occupies the lower 2 m. The clay content gradually increases, and the occurrence of sand (either foraminifer ooze or lithic fragments) decreases with depth in the hole. The magnetic susceptibility increases in intervals with increasing clay content, bioturbation, and sand layers. Foraminifer oozes are characterized by very low susceptibility values. The magnetic susceptibility increases sharply at the Subunit IA/IB contact and remains high in Subunit IB. Density and sonic velocity show normal gradients in the upper 10–20 m, below which high values correlate with sand layers.

The composition of interstitial waters at Site 1074 generally show only minor variations as the result of diagenetic alteration. There is little evidence of microbial decomposition of organic matter, suggesting low organic-matter content in the sediments. Potassium and H_4SiO_4 increase at the base of Subunit IA, indicating a source for these constituents in the clay-rich sediments (Subunit IB) at the base of the sedimentary section. There appears to be little diffusive exchange between sedimentary and basement pore fluids, perhaps as a result of the presumably low-permeability basal clay. Downhole temperatures measured on Cores 3H through 6H are consistent with purely conductive heat transfer. Thus, there is no evidence for fluids vertically advecting through the sediment column at Site 1074. This observation supports the model proposed by Langseth et al. (1984, 1992) that fluid circulation is confined to the basement beneath the sediment pond and that heat transfer through the sediments is predominantly conductive.

BACKGROUND AND OBJECTIVES

When the logging and Circulation Obviation Retrofit Kit (CORK) operations at Hole 395A were successfully completed ahead of schedule, ~2 days of time became available for other operations during Leg 174B. This was applied toward the contingency program already approved for Leg 174B, coring the sediments of North Pond. The objectives of the contingency program, like those of the primary program at Hole 395A, were primarily hydrogeological. However, it should be noted that the advanced hydraulic piston corer (APC) had not been developed when Site 395 was cored during Ocean Drilling Program (ODP) Leg 45, and the sediments at the site were not recovered well with the rotary core barrel (RCB) system. Thus, simply recovering a representative sediment section from North Pond with the ODP system was also of great interest. Although the small scientific party of Leg 174B was not staffed for sedimentological studies, the party of JANUS observers covered the basic needs, and they were enthusiastically drafted into scientific action at Site 1074.

With less than 24 hr of actual coring time available, it was decided to focus on a site ~4 km northwest of Hole 395A, where the detailed survey by Langseth et al. (1992) showed the highest heat flow in North Pond. The location of Site 1074 is near the northwest edge of North Pond, where a basement ridge emerges from the sediments (Fig. 1). Site 1074 and the peak heat-flow values lie ~500 m northwest of single-channel seismic Line A–A′ from Langseth et al. (1992; Fig. 2). If the site location is projected onto the seismic line, it would lie just southwest of the prominent basement ridge midway along the line, where sediment thickness is ~0.5 s; thus, we expected to core ~50 m of sediments at Site 1074.

The hydrogeological objective at Site 1074 was to investigate the cause of the local heat-flow high. In particular, we hoped to determine between two hypotheses for the high surface heat flow involving fluid flow in different ways: (1) that the high heat flow is caused by pore-fluid advection up through the sediments, or (2) that heat transfer through the sediments is predominantly conductive, with surface heat flow inversely proportional to sediment thickness above a basement held nearly isothermal by strong lateral fluid flow in basement, as modeled by Langseth et al. (1984, 1992). To address this issue, we emphasized (1) resolution of geochemistry of pore fluids, and (2) downhole temperature measurements using the Adara and Davis-Villinger Temperature Probe (DVTP) tools. A temperature tool was deployed at or after every core except the first two, where the probes generally cannot be held stable enough for valid measurements.

OPERATIONS

Hole 1074A

After successful deployment of the CORK in Hole 395A, over a day, almost two days of operational time was still available. This extra time was applied to the contingency plan for Leg 174B, coring the

[1]Becker, K., Malone, M.J., et al., 1998. *Proc. ODP, Init. Repts.*, 174B: College Station, TX (Ocean Drilling Program).
[2]Shipboard Scientific Party is given in the list preceding the Table of Contents.

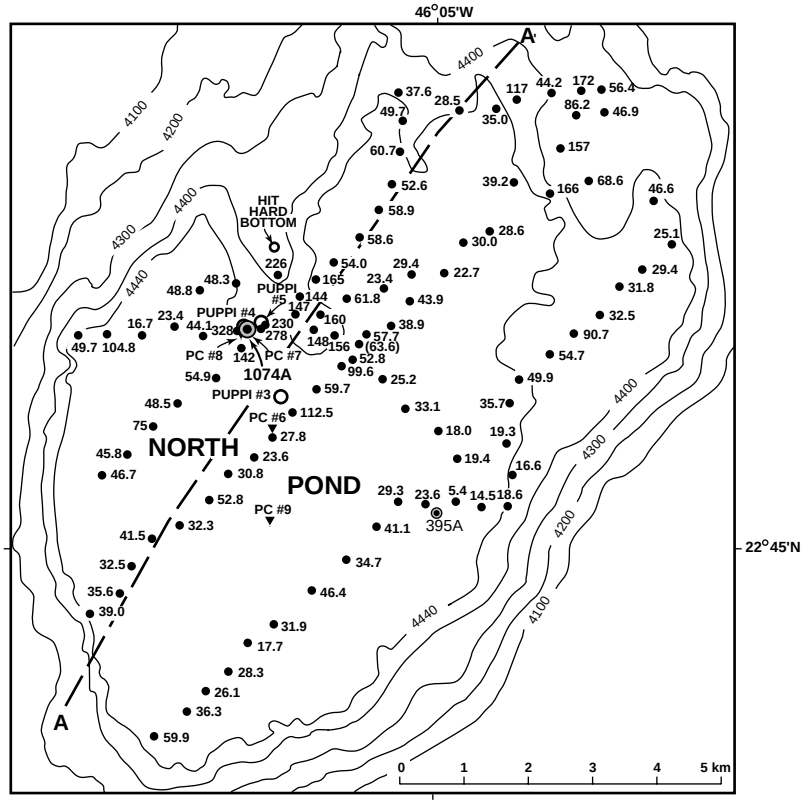

Figure 1. Locations of heat-flow measurements, pup-up pore pressure instrument (PUPPI) deployments, piston cores, and Hole 395A in North Pond. Heat-flow values are given in mW/m^2 (from Langseth et al., 1992).

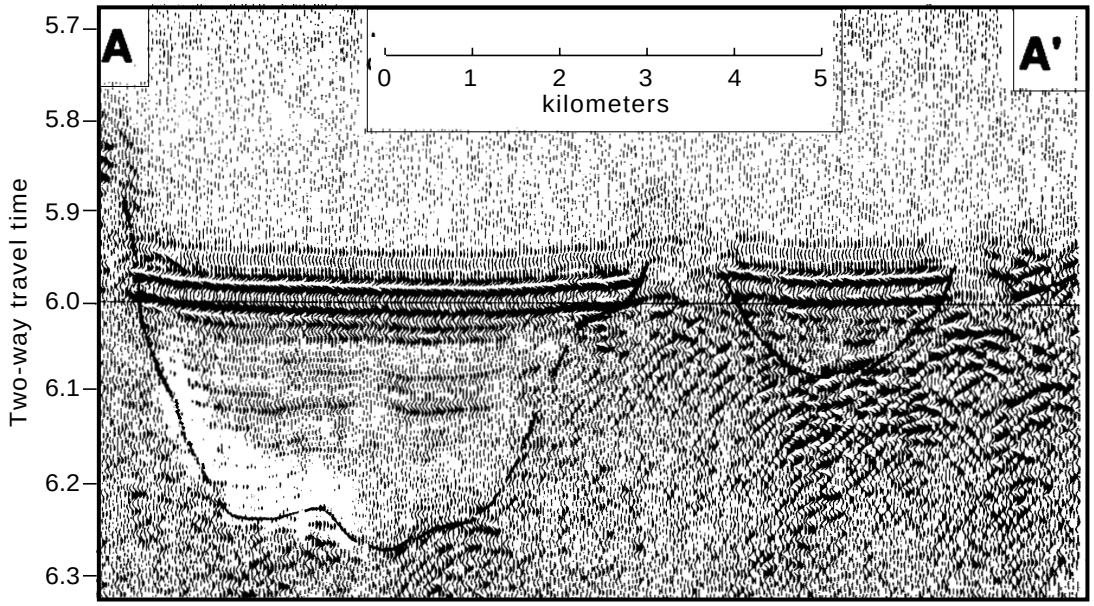

Figure 2. Single-channel seismic section across North Pond along Line A–A′, as shown in Figure 1 (from Langseth et al., 1992).

sediments of North Pond. The ship was moved 2.4 nmi (4.44 km) northwest in dynamic positioning (DP) mode, and a beacon was deployed. An APC BHA was assembled, and a brief survey with the vibration-isolated television (VIT) frame was conducted to confirm the seafloor condition, which was flat and featureless. Based on recovery of the mudline core, the water depth was 4445.5 mbsl. Hole 1074A was spudded at 1315 hr, 1 August, and APC Cores 174B-1074A-1H through 7H were taken from 0 to 63.5 mbsf (103.6% recovery; Table 1). Adara heat-flow measurements were made on Cores 3H through 6H, and the Tensor tool was run on Cores 3H through 7H. The inner core barrel that was used to cut Cores 2H, 4H, and 6H contained a 3-m long nonmagnetic section (see "Appendix" section on CD-ROM, back pocket, this volume). Core 7H was a partial stroke, encountering a hard layer (basalt clast) with increased torque at 8.5 m (62.5 mbsf); hence, the lower 1.53 m of Core 7H is probably highly disturbed (flow-in). The hole was drilled down to 63.5 mbsf, 1.5 m below the APC-shoe penetration. We switched to the extended core barrel (XCB) coring system and Core 8X was cut from 63.5 to 69.5 mbsf (Table 1). High torque stalled the rotary repeatedly, requiring increased pump rates, a mud sweep, and repeated reaming of the hole.

Table 1. Site 1074 expanded coring summary.

Core	Date (Aug. 1997)	Time (UTC)	Depth (mbsf)	Length cored (m)	Length recovered (m)	Recovery (%)	Section	Liner length (m)	Curated length (m)	Top (mbsf)	Bottom (mbsf)	Samples
174B-1074A-												
1H	1	1550	0.0-6.5	6.5	6.41	98.6						
							1	1.50	1.50	0.00	1.50	IW
							2	1.50	1.50	1.50	3.00	IW
							3	1.50	1.50	3.00	4.50	IW
							4	1.00	1.00	4.50	5.50	
							5	0.73	0.73	5.50	6.23	
							CC(w/5)	0.18	0.18	6.23	6.41	PAL
							Total:	6.41	6.41			
2H	1	1805	6.5-16.0	9.5	9.93	104.5						
							1	1.50	1.50	6.50	8.00	IW
							2	1.50	1.50	8.00	9.50	
							3	1.50	1.50	9.50	11.00	IW
							4	1.50	1.50	11.00	12.50	
							5	1.50	1.50	12.50	14.00	IW
							6	1.50	1.50	14.00	15.50	
							7	0.77	0.77	15.50	16.27	
							CC(w/7)	0.16	0.16	16.27	16.43	PAL
							Total:	9.93	9.93			
3H	1	1935	16.0-25.5	9.5	10.18	107.2						
							1	1.50	1.50	16.00	17.50	IW
							2	1.50	1.50	17.50	19.00	
							3	1.50	1.50	19.00	20.50	IW
							4	1.50	1.50	20.50	22.00	
							5	1.50	1.50	22.00	23.50	IW
							6	1.50	1.50	23.50	25.00	
							7	0.87	0.87	25.00	25.87	
							CC(w/7)	0.31	0.31	25.87	26.18	PAL
							Total:	10.18	10.18			
4H	1	2055	25.5-35.0	9.5	9.71	102.2						
							1	1.50	1.50	25.50	27.00	IW
							2	1.50	1.50	27.00	28.50	
							3	1.50	1.50	28.50	30.00	IW
							4	1.50	1.50	30.00	31.50	
							5	1.50	1.50	31.50	33.00	IW
							6	1.50	1.50	33.00	34.50	
							7	0.45	0.45	34.50	34.95	
							CC(w/7)	0.26	0.26	34.95	35.21	PAL
							Total:	9.71	9.71			
5H	1	2220	35.0-44.5	9.5	9.64	101.5						
							1	1.50	1.50	35.00	36.50	IW
							2	1.50	1.50	36.50	38.00	
							3	1.50	1.50	38.00	39.50	
							4	1.50	1.50	39.50	41.00	
							5	1.50	1.50	41.00	42.50	IW
							6	1.50	1.50	42.50	44.00	
							7	0.48	0.48	44.00	44.48	
							CC(w/7)	0.16	0.16	44.48	44.64	PAL
							Total:	9.64	9.64			
6H	1	2350	44.5-54.0	9.5	9.86	103.8						
							1	1.50	1.50	44.50	46.00	
							2	1.50	1.50	46.00	47.50	IW
							3	1.50	1.50	47.50	49.00	
							4	1.50	1.50	49.00	50.50	
							5	1.50	1.50	50.50	52.00	IW
							6	1.50	1.50	52.00	53.50	
							7	0.54	0.54	53.50	54.04	
							CC(w/7)	0.32	0.32	54.04	54.36	PAL
							Total:	9.86	9.86			
7H	2	0100	54.0-63.5	9.5	10.03	105.6						
							1	1.50	1.50	54.00	55.50	
							2	1.50	1.50	55.50	57.00	IW
							3	1.50	1.50	57.00	58.50	
							4	1.50	1.50	58.50	60.00	
							5	1.50	1.50	60.00	61.50	IW
							6	1.50	1.50	61.50	63.00	
							7	0.87	0.87	63.00	63.87	
							CC(w/7)	0.16	0.16	63.87	64.03	PAL
							Total:	10.03	10.03			
8X	2	0700	63.5-69.5	6.0	0.58	9.7						
							1	0.58	1.02	63.50	64.52	
							Total:	0.58	1.02			
			Coring totals:	69.5	66.34	95.5						

Notes: UTC = Universal Time Coordinated. IW = interstitial water, PAL = paleontology. Water depth from sea surface = 4445.4 m. Position of Hole 1074A = 22°46.8326′N, 46°6.7398′W.

Despite the hole problems, Core 8X was retrieved with 0.58 m of basalt (9.7% recovery).

During the connection after Core 8X, the beacon signal was lost for positioning. Shortly thereafter the internet connection to the GPS-Glonass and global positioning (GPS) systems in the underway lab, the positioning back-up reference, was also lost. The drill pipe was pulled, and the ship was held to a 45-m maximum excursion using dead reckoning until the bit cleared the seafloor at 0520 hr on 2 August, ending Hole 1074A.

Transit to Las Palmas

The 1726 nmi (3197 km) sea voyage to Las Palmas was completed in 166 hr at an average speed of 10.4 kt, which included 8.75 hr at 6 kt to conduct seismic streamer tests over the Madeira/Cape Verde abyssal plain. The first line was ashore at 1500 hr on 9 August, officially ending Leg 174B.

LITHOSTRATIGRAPHY

Sixty-four meters of sediment and 0.58 m of basalt were recovered at the single hole drilled at Site 1074. A total of 8 cores were recovered: Cores 174B-1074A-1H through 7H contain sediments, and Core 8X is basalt. Two lithologic units were defined: Unit I contains nannofossil ooze with varying amounts of foraminifers, clay, radiolarians and sand, and nannofossil clay, overlying Unit II, a unit of aphyric basalt. The sedimentary Unit I was divided into two subunits based on the magnetic susceptibility record, clay content, and the presence or absence of graded sand layers. The clay content gradually increases, and the occurrence of sand (either foraminifer ooze or lithic fragments) decreases with depth in the hole. The magnetic susceptibility increases sharply at the Subunit IA/IB contact and remains high in Subunit IB. A summary of the major lithologic units is presented in Figure 3.

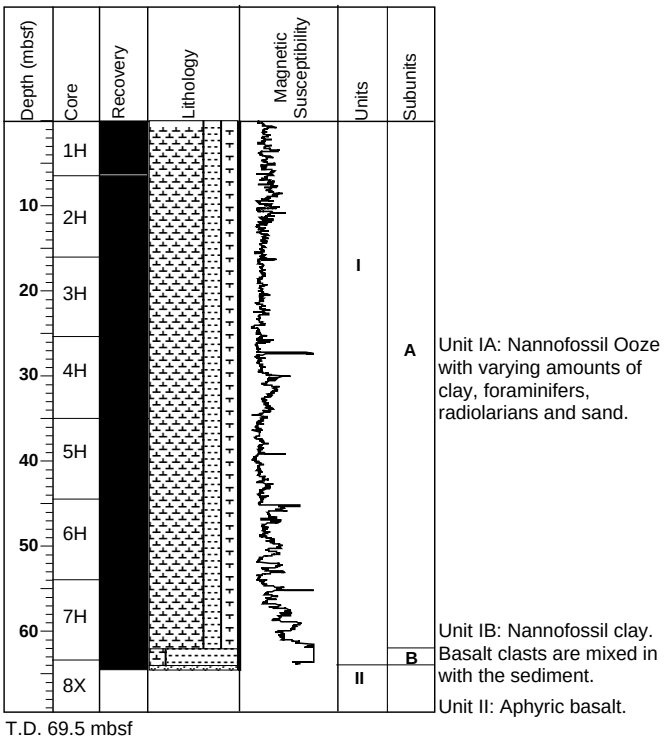

Figure 3. Generalized lithology of the sedimentary units recovered at Hole 1074A. T.D. = total depth.

Recovery was excellent in the sedimentary section. However, many intervals of the core were disturbed by the drilling process. These intervals were at the top of each core and within the sandy, unconsolidated layers.

These cores were collected as part of a contingency plan after a CORK was installed in Hole 395; there are no biostratigraphic data available to date the sediments, because the personnel on board could not perform the analyses. Paleomagnetic data were collected; however, a drilling-induced magnetic overprint prevented development of a shipboard magnetic stratigraphy (see "Paleomagnetism" section, this chapter).

Description of Lithologic Units

Lithologic Unit I

Interval: Cores 174B-1074A-1H through 174B-1074A-7H
Age: not determined
Depth: 0–63.5 mbsf

Unit I is composed of pelagic sediment, primarily nannofossil ooze, which is mixed with varying amounts of clay, foraminifers, radiolarians, and sand. This lithology changes abruptly to clay near the bottom of the sedimentary column. The upper part of Unit I is moderately bioturbated in some intervals, and there are many layers of foraminifer ooze and sand.

Subunit IA

Interval: Core 174B-1074A-1H through Section 174B-1074A-7H-6, 0 cm
Age: not determined
Depth: 0–61.50 mbsf

The primary lithology is nannofossil ooze, which contains varying amounts of clay, foraminifers, and radiolarians. Generally this unit alternates between light layers with higher calcium carbonate content and darker layers that contain more clay. There are intervals of bioturbated sediment, characterized by light carbonate mottles and burrows within clayey nannofossil ooze.

Two minor lithologies that only occur in this subunit are sand and foraminifer ooze. The sand units are composed of lithic fragments, primarily basalt, but also plagioclase, other mineral particles, and opaque minerals. Both the foraminifer ooze and the sand layers display normally graded bedding, sharp bottom contacts, and gradational, and often bioturbated, upper contacts. In general, the sand and foraminifer ooze layers were very disturbed during the coring process and are quite soupy. Mud clasts were observed in intervals 174B-1074A-1H-3, 42–44 cm; 3H-2, 69–70 cm; and 7H-3, 83–85 cm. Manganese micronodules are present throughout Subunit IA.

Bulk X-ray diffraction (XRD) analysis indicates that the aluminosilicate mineral composition does not vary significantly between samples. Mineral phases identified by XRD include calcite, illite, chlorite, and plagioclase.

Subunit IB

Interval: Sections 174B-1074A-7H-6, 0 cm, through 174B-1074A-7H-CC
Age: not determined
Depth: 61.50–63.50 mbsf

Subunit IB is composed of red clay with only ~20% carbonate. This clay interval is disturbed by the drilling process; flow-in affects about two thirds of the subunit. There is a 6-cm basalt clast in Sample 174B-1074A-7H-7, 28 cm, and many small (<1 cm) basalt clasts present throughout the lower part of the subunit. There is one interval of carbonate-rich sediment in this unit, and the carbonate is bioturbated.

Lithologic Unit II

Interval: Section 174B-1074A-8X-1
Age: not determined
Depth: 63.5–69.5

The rock recovered at Section 174B-1074A-8X-1 consists mainly of pebble- to hand-sized specimens of slightly altered aphyric basalt. The groundmass consists of interlocking laths of plagioclase with anhedral mafic minerals. There are a few very small amygdules coated with zeolite in otherwise massive basalt. The grain size (~0.5 mm) of most of the ground mass indicates that the basalt is probably from the interior of a relatively thick pillow or basalt flow.

Discussion

The Subunit IA sediments at Site 1074 reflect periods of pelagic sedimentation interrupted by abrupt deposition of both foraminifer oozes and normally graded sand layers. The presence of sharp bottom contacts and graded bedding as well as the occurrence of mud clasts in some regions indicate that these coarse-grained intervals are the result of downslope transport to Site 1074. In contrast, the Subunit IB clay shows little evidence of episodic sedimentation and represents a period of undisturbed sedimentation.

PALEOMAGNETISM

Introduction

Paleomagnetic observations were made on the first seven cores recovered from Hole 1074A, both as a part of the magnetic experiments described in the "Appendix" section (CD-ROM, back pocket, this volume) and to determine the magnetostratigraphy of the site. The initial drilling at Site 395 had been by RCB, which precluded paleomagnetic measurements in the sediments, so that the APC cores obtained on this leg provided the first opportunity to establish the magnetostratigraphy in North Pond.

Methods

Archive halves of the cores were measured with the 2G cryogenic magnetometer and demagnetized at steps of 5, 10, 15, 20, and 30 mT. The results were analyzed by principal component analysis and line fitting of Zijderveld plots, using shipboard software. Discrete samples were also measured and analyzed in the same way. In addition, their demagnetization characteristics were compared with those of anhysteretic remanent magnetization (ARM) and saturation isothermal remanent magnetization (IRMs).

Results

A plot of inclination as a function of depth is given for the 20-mT demagnetization measurements in Figure 4. The record of uncorrected declination is of little interest, because it is dominated by values close to zero, so that it appears that the radial horizontal component has obscured this record. There is some indication of a possible magnetostratigraphic record in the inclination, although the majority of the inclination values are too steep for the site latitude and indicate vertical contamination. Until either u-channels, or discrete samples, are measured onshore, the calls of chrons must be regarded as preliminary.

From ~6.5 to 16 mbsf, the inclination is dominantly negative and probably represents Chron 1r. Cores 174B-1074A-3H and 4H exhibit a trend from high positive inclination at 16 mbsf to high negative inclination, which terminates with a rapid change to a positive inclination at about 31 mbsf. Whether this is a reflection of polarity changes or an artifact is not clear. If it is at least partially a geomagnetic signal, then the strong positive should be the Olduvai (i.e., Chron 2), followed by Chron 2r. From 31 to 52 mbsf, there is a dominantly positive inclination with a number of minor excursions to negative values, which may be the Gauss (Chron 3). Below this depth, a final length of negative inclination could be the Gilbert. These interpretations should, however, be regarded with caution, because some of the inclination boundaries coincide with intensity peaks in the record that may themselves be related to barrel magnetizations, as is discussed in more detail in the "Appendix" (CD-ROM, back pocket, this volume).

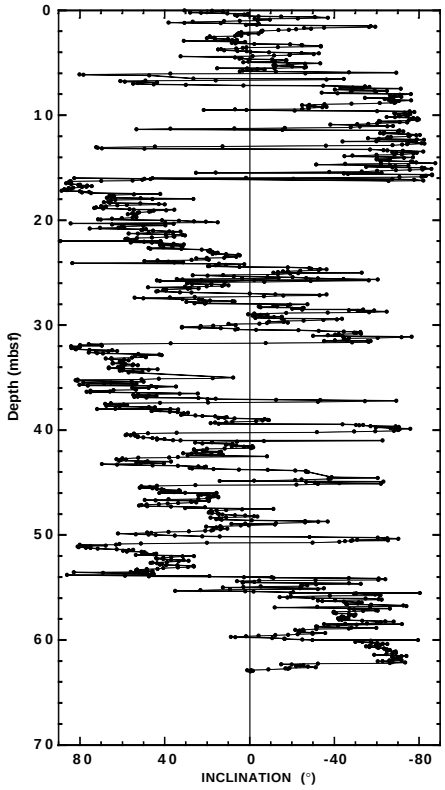

Figure 4. Inclination for Cores 174B-1074A-1H through 7H after demagnetization to 20 mT.

Analysis of the demagnetization of individual discrete samples yielded some well-defined directions (Fig. 5), but the majority were poorly defined with no clear endpoint or convergence to the origin (Fig. 5). Many of these latter samples follow a rough great circle pattern suggestive of two components. In some cases, each of these components appears to be steeply inclined, but of opposite polarity. Comparison of the demagnetization characteristics of the natural remanent magnetization (NRM) with the ARM and IRM yield plots that are indicative of some contamination, but nevertheless at higher demagnetization fields the ratio of NRM to IRM of about 1:1000 was appropriate for a depositional remanence (Fig. 6).

The combination of the radial horizontal and vertical contamination have made the interpretation of magnetostratigraphy at this site problematical. Thus, the declinations are largely near zero, and the inclinations are frequently oversteep for the site latitude. The Matuyama appears to be recorded so that we see Chron 1r reasonably convincingly, and below that we may be seeing Chrons 2, 2r, 3, and 3r. However, definitive magnetostratigraphy must await shore-based studies.

INORGANIC GEOCHEMISTRY

Eighteen whole-round samples were taken from Hole 1074A for high-resolution, interstitial water analyses. One of the primary objec-

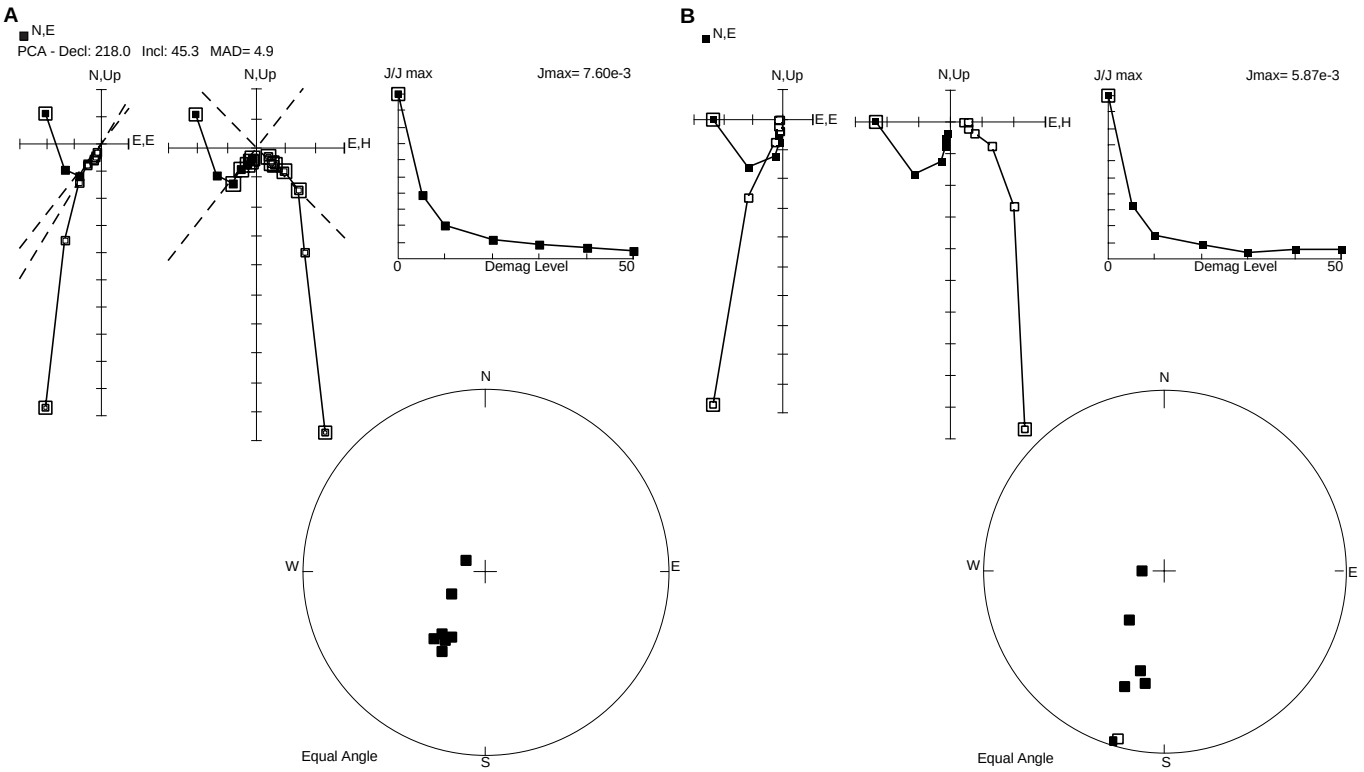

Figure 5. Examples of demagnetization analysis of discrete samples. **A.** Sample 174B-1074A-4H-4, 71–73 cm. **B.** Sample 174B-1074A-4H-4, 66–68 cm.

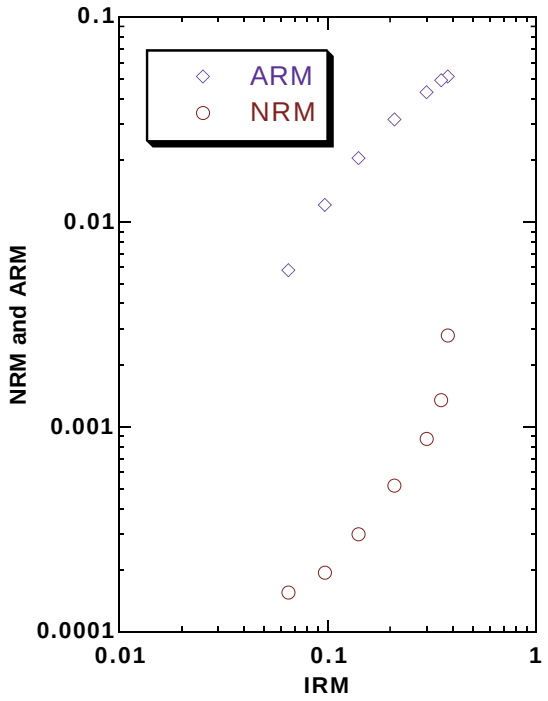

Figure 6. Comparison of demagnetization characteristics of NRM, ARM, and IRM for Sample 174B-1074A-4H-2, 66–68 cm.

tives of Site 1074 was to discriminate between two hypotheses for the high surface heat flow that involves fluid flow in different ways: (1) the high heat flow is caused by pore-fluid advection up through the sediments; or (2) the heat transfer through the sediments is predominantly conductive, with surface heat flow inversely proportional to sediment thickness above a basement held nearly isothermal by strong lateral fluid flow in basement, as modeled by Langseth et al. (1984, 1992).

Preliminary Interpretations

Results from shipboard interstitial water analyses are reported in Table 2 and Figure 7. The uniform values of SO_4^{2-}, alkalinity, and the lack of detectable NH_4^+ throughout the sedimentary section suggest minimal bacterial activity and low organic-matter contents (Table 2; Fig. 7). The increase in Sr^{2+} concentrations with depth is the result of minor diagenetic recrystallization of biogenic carbonates in pelagic, carbonate-rich (low-Mg calcite) sediments (e.g., Baker et al., 1982). Despite the presence of radiolarian-rich intervals in the sediments, H_4SiO_4 concentrations are only slightly elevated relative to bottom-water values. The lack of significant diagenetic alteration of carbonate and siliceous microfossils that is implied by the pore-water composition is consistent with the good preservation observed in smear slides from lithologic Subunit IA (see "Lithostratigraphy" section, this chapter) and the unconsolidated state of the sediments. A corresponding increase in H_4SiO_4 (8.3 times higher than bottom water) and K^+ (16% increase over bottom water) occurs above the Subunit IA/IB boundary. The Subunit IA/IB boundary is defined by a sharp increase in clay content from a clayey nannofossil ooze to a nannofossil clay (see "Lithostratigraphy" section, this chapter). The increase in H_4SiO_4 and K^+ immediately above the clay-rich sediments suggests diffusional exchange with a source of H_4SiO_4 and K^+ in the clay.

Slightly elevated Cl^- and $\delta^{18}O$ values, relative to present-day seawater concentrations previously observed in pore fluids from nearby Site 395, were attributed to the general increase in seawater salinity during glacial advances over the past million years (Lawrence et al.,

Table 2. Interstitial water data for Site 1074.

Core, section, interval (cm)	Depth (mbsf)	pH	Alkalinity (mM)	Salinity	Cl^- (mM)	SO_4^{2-} (mM)	Sr^{2+} (μM)	Mg^{2+} (mM)	Ca^{2+} (mM)	K^+ (mM)	H_4SiO_4 (μM)
174A-1074A-											
1H-1, 140-150	1.4	7.68	2.69	35.0	559	27.72	88	53.35	10.32	11.65	114
1H-2, 140-150	2.9	7.64	2.63	35.0	557	28.22	93	52.39	10.39	11.98	135
1H-3, 140-150	4.4	7.81	2.69	35.0	558	27.42	93	52.24	10.27	11.72	132
2H-1, 140-150	7.9	7.58	2.91	35.0	556	28.63	96	52.62	10.63	11.85	123
2H-3, 140-150	10.9	7.75	2.72	35.0	556	27.94	98	52.68	10.56	11.98	120
2H-5, 140-150	13.9	7.81	2.80	35.0	557	27.17	100	52.72	10.50	11.44	105
3H-1, 140-150	17.4	7.68	2.79	35.0	559	27.73	105	52.27	10.77	11.80	108
3H-3, 140-150	20.4	7.77	2.72	35.0	558	28.69	108	51.99	10.28	11.48	111
3H-5, 140-150	23.4	7.81	2.68	36.0	560	27.76	110	52.60	10.29	11.41	99
4H-1, 140-150	26.9	7.81	2.74	36.0	563	29.00	114	53.37	10.82	10.76	78
4H-3, 140-150	29.9	7.75	2.76	36.0	563	28.19	114	53.34	10.31	11.03	90
4H-5, 140-150	32.9	7.81	2.74	36.0	562	30.40	116	52.22	10.52	10.99	96
5H-1, 140-150	36.4	7.81	2.56	36.0	564	28.98	114	52.91	10.46	11.09	93
5H-5, 140-150	42.4	7.68	2.53	36.0	564	29.14	112	52.47	10.28	11.37	93
6H-2, 140-150	47.4	7.68	2.54	36.0	564	29.02	112	52.83	10.22	11.30	102
6H-5, 140-150	51.9	7.68	2.50	36.0	563	29.24	110	53.36	10.42	11.01	96
7H-2, 140-150	56.9	7.62	2.49	36.0	561	28.15	108	52.24	10.04	11.59	126
7H-5, 140-150	61.4	7.68	2.27	36.0	556	28.83	101	51.82	10.13	12.08	208

Note: NH_4^+ determinations were attempted, but concentrations were very near or below detection limits.

1979; McDuff, 1984). The Cl^- profile at Site 1074 decreases slightly near the sediment/seawater interface and then increases to 564 mM (~1% above bottom-water concentrations) at 42 mbsf. The interval of slightly elevated Cl^- concentrations may reflect relict Pleistocene values partially modified by diffusional processes. Below the maximum, Cl^- concentrations decrease to a minimum value of 556 mM directly above the Subunit IA/IB boundary.

Concentration gradients in Ca^{2+}, Mg^{2+}, and K^+ in settings where pelagic sediments overlie basaltic basement are predominately the result of alteration of volcanic matter dispersed in the sediments as well as diffusive exchange with altered basaltic basement (e.g., Gieskes and Lawrence, 1981). The gradients are typified by decreases in Mg^{2+} and K^+ and increases in Ca^{2+}. Although there is a slight decrease in Mg^{2+} concentrations at depth in Hole 1074A, no corresponding increase in Ca^{2+} or decrease in K^+ is apparent. By contrast, K^+ increases toward the base of the sedimentary section. These data, combined with the limited Ca^{2+}, Mg^{2+}, and $\delta^{18}O$ pore-water compositions from Site 395 (Lawrence et al., 1979), suggest that there is little diffusive exchange occurring between the basement and overlying sediments, perhaps inhibited by Subunit IB clay-rich sediments.

If fluid circulating in the basement is relatively unaltered seawater rather than fluid with an altered basaltic signature, then the strong Ca^{2+}, Mg^{2+}, and K^+ gradients described above would not be expected. However, it has previously been observed that when unaltered seawater is laterally advecting through basement and there is diffusive exchange between basement fluids and sedimentary pore waters, then the shape of interstitial water profiles show concentrations reverting back to seawater-like values (Baker et al., 1991). It is more difficult to determine if this process is occurring at Hole 1074A because many pore-water constituents remain relatively unchanged from seawater values. Two ions, Cl^- and Sr^{2+}, return close to bottom-water values at the base of the sedimentary section. However, K^+ and H_4SiO_4 abruptly increase to values greater than seawater and in the opposite direction than would be expected if there were basaltic alteration. These observations also suggest that there is little diffusive exchange with basement.

The composition of interstitial waters also shows no evidence of vertical advection of fluids through the sediment column. Systematic curvature of profiles that might be expected if there was slow, upward seepage of basement fluids (e.g., Davis, Fisher, Firth, et al., 1997) are not observed. Furthermore, the aforementioned diffusive gradients (Cl^-, Sr^{2+}, K^+, and H_4SiO_4) clearly could not be maintained if there was a significant, vigorous, vertical advection of fluids through the sediments.

In summary, the composition of interstitial waters at Site 1074 generally shows only minor variations as the result of diagenetic alteration. There is little evidence of microbial decomposition of organic matter, suggesting low organic-matter content in the sediments. Potassium and H_4SiO_4 increase at the base of Subunit IA, indicating a source for these constituents in the clay-rich sediments (Subunit IB) at the base of the sedimentary section. There appears to be little diffusive exchange between sedimentary and basement pore fluids, perhaps as a result of the presumably low-permeability basal clay. There is no evidence for fluids vertically advecting through the sediment column at Site 1074. This observation supports the model proposed by Langseth et al. (1984, 1992) that fluid circulation is confined to the basement and that heat transfer through the sediments is predominantly conductive.

PHYSICAL PROPERTIES/HEAT FLOW

Multisensor Track

The multisensor track (MST) was used to measure bulk density, acoustic compressional-wave velocity, and magnetic susceptibility on all APC cores in Hole 1074A (Fig. 8; Table 3 on CD-ROM, back pocket, this volume). In the upper 19 mbsf, bulk density shows a normal consolidation trend, increasing with depth. Below this depth, the bulk density values do not show trends with depth, but vary as a function of grain size. Higher density values are associated with coarser sediments, and lower values represent finer grained intervals. Discrete values of bulk density, determined from samples using the wet mass and volume, show good correlation with the gamma-ray attenuation porosity evaluator (GRAPE)–determined measurements (Fig. 8).

Magnetic susceptibility measurements respond to bulk density and compositional changes. In the upper 45 mbsf, susceptibility values are generally low, but higher values occur over short depth intervals and correspond with coarser grained lithic intervals. At the base of the hole, susceptibility measurements increase with depth, corresponding to an increase in the lithic fraction and clasts.

Acoustic velocity increases from seawater values at the seafloor to >1500 m/s at 12 mbsf. Below this depth, velocity does not increase with depth, but higher velocity intervals (~1600 m/s) occur throughout and are associated with coarser grained intervals. When compared with the susceptibility record, high-velocity values correspond to coarse-grained intervals, whereas susceptibility corresponds only to nonforaminifer coarse-grained intervals.

Thermal Conductivity

Thermal conductivity was measured using the needle probe method on every other section (see “Explanatory Notes” chapter, this volume). The measurements are within the normal range of values for

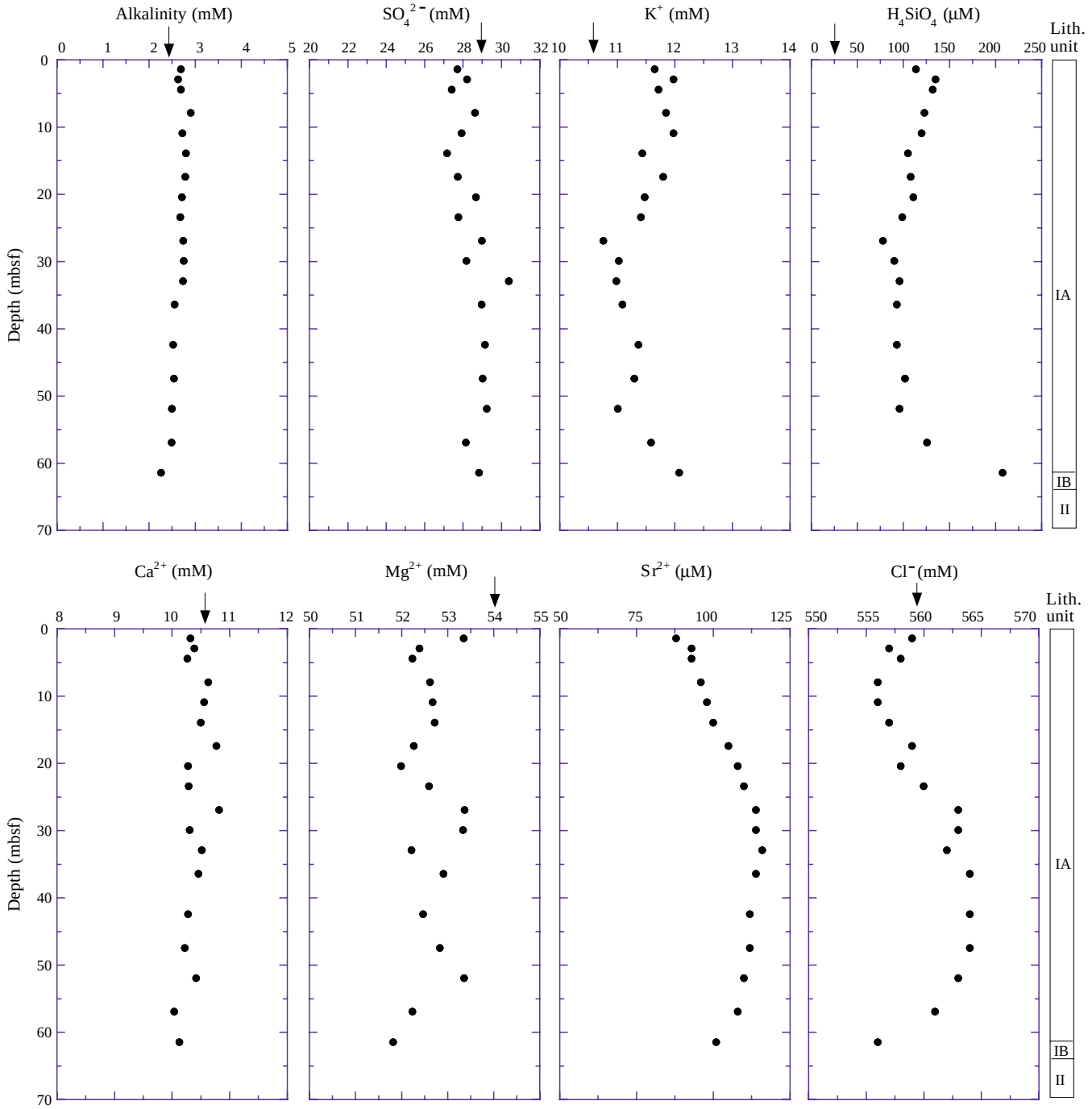

Figure 7. Concentration/depth profiles of interstitial water at Site 1074. Arrows = bottom-water concentrations reported by McDuff (1984) at nearby Site 395. Lithologic units are from the "Lithostratigraphy" section, this chapter.

soft marine sediments (Fig. 9; Table 4). With the exception of one measurement, the values are slightly lower than the value used by Langseth et al. (1992) for heat-flow calculations in this area (North Pond; 0.9–1.2 W/[m·K]).

Temperature and Heat Flow

Downhole temperatures were made with the Adara temperature tool at four depths in Hole 1074A. The instrument functioned well on all runs. The Adara temperature data were reduced for in situ values following the procedures outlined in the "Explanatory Notes" chapter (this volume). The individual temperature measurement runs are shown in Figure 10. The temperature data were combined with the thermal conductivity measurements to calculate heat flow. Thermal conductivity values, although scattered, are relatively uniform with depth having an average value of 1.1 W/(m·K). The standard deviation is 0.1 W/(m·K). A linear regression was fit to the temperature-depth data, constrained to pass through the bottom-water temperature (Fig. 11). Heat flow, calculated as the product of the slope of the linear regression and the average thermal conductivity, is 72 mW/m^2.

REFERENCES

Baker, P.A., Gieskes, J.M., and Elderfield, H., 1982. Diagenesis of carbonates in deep-sea sediments: evidence from Sr^{2+}/Ca^{2+} ratios and interstitial dissolved Sr^{2+} data. *J. Sediment. Petrol.*, 52:71–82.

Baker, P.A., Stout, P.M., Kastner, M., and Elderfield, H., 1991. Large-scale lateral advection of seawater through oceanic crust in the central equatorial Pacific. *Earth Planet. Sci. Lett.*, 105:522–533.

Davis, E.E., Fisher, A.T., Firth, J.V., et al., 1997. *Proc. ODP, Init. Repts*., 168: College Station, TX (Ocean Drilling Program).

Gieskes, J.M., and Lawrence, J.R., 1981. Alteration of volcanic matter in deep-sea sediments: evidence from the chemical composition of interstitial waters from deep sea drilling cores. *Geochim. Cosmochim. Acta*, 45:1687–1703.

Langseth, M.G., Becker, K., Von Herzen, R.P., and Schultheiss, P., 1992. Heat and fluid flux through the sediment on the western flank of the Mid-Atlantic Ridge: a hydrological study of North Pond. *Geophys. Res. Lett.*, 19:517–520.

Langseth, M.G., Hyndman, R., Becker, K., Hickman, S.H., and Salisbury, M., 1984. The hydrogeologogical regime of isolated sediment ponds in mid-oceanic ridges. *In* Hyndman, R.D., Salisbury, M.H., et al., *Init. Repts. DSDP*, 78 (Pt. 2): Washington (U.S. Govt. Printing Office), 825–837.

Lawrence, J.R., Drever, J.J., and Kastner, M., 1979. Low temperature alteration of basalts predominates at Site 395. *In* Melson, W.G., Rabinowitz, P.D., et al., *Init. Repts. DSDP*, 45: Washington (U.S. Govt. Printing Office), 609–612.

McDuff, R.E., 1984. The chemistry of interstitial waters from the upper ocean crust, Site 395, Deep Sea Drilling Project Leg 78B. *In* Hyndman, R.D., Salisbury, M.H., et al., *Init. Repts. DSDP*, 78B: Washington (U.S. Govt. Printing Office), 795–799.

Ms 174BIR-103

NOTE: Core-description forms (“barrel sheets”) and core photographs can be found in Section 3, beginning on page 39. See Table of Contents for material contained on CD-ROM.

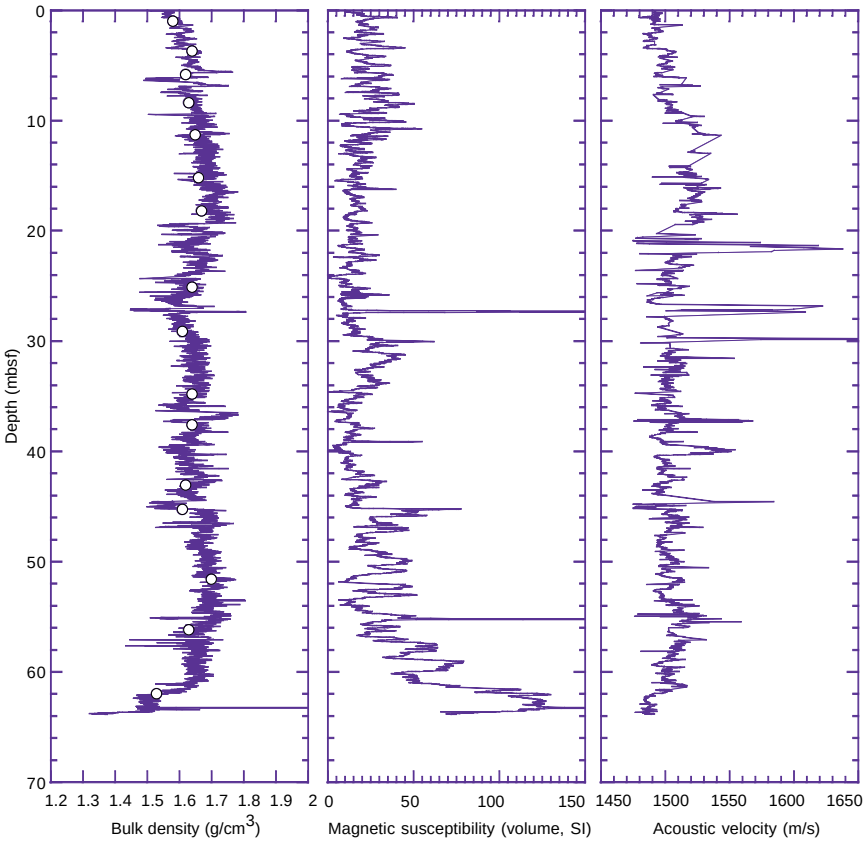

Figure 8. Bulk density (determined using the GRAPE), magnetic susceptibility, and acoustic compressional wave velocity vs. depth for Hole 1074A. The open circles in the bulk density plot are discrete measurements of bulk density that correlate well with the GRAPE data.

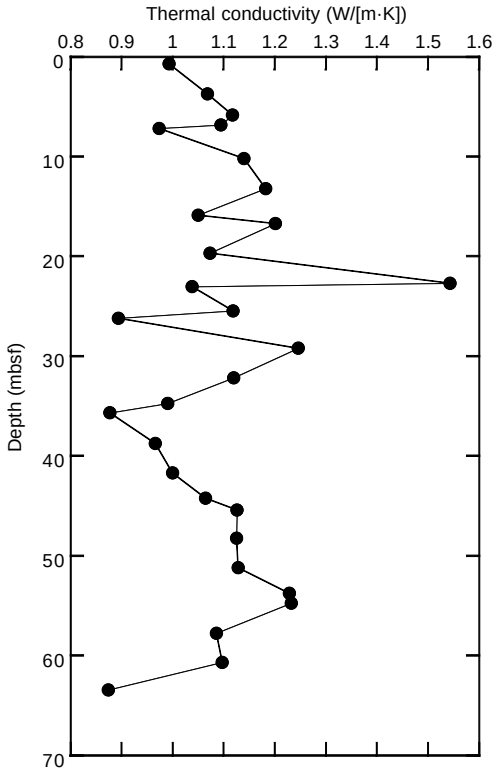

Figure 9. Thermal conductivity measured with a needle probe on whole cores from Hole 1074A vs. depth.

Table 4. Thermal conductivity values measured with a needle probe on whole core from Hole 1074A vs. depth.

Core, section, interval (cm)	Depth (mbsf)	Thermal conductivity (W/[m·K])
174B-1074A-		
1H-1, 70-70.1	0.70	0.994
1H-3, 70-70.1	3.70	1.069
1H-5, 36-36.1	5.86	1.118
2H-1, 35-35.1	6.85	1.095
2H-1, 70-70.1	7.20	0.974
2H-3, 70-70.1	10.20	1.140
2H-5, 70-70.1	13.20	1.183
2H-7, 38-38.1	15.88	1.050
3H-1, 70-70.1	16.70	1.095
3H-3, 70-70.1	19.70	1.074
3H-5, 70-70.1	22.70	1.543
3H-5, 105-105.1	23.05	1.039
3H-7, 44-44.1	25.44	1.119
4H-1, 70-70.1	26.20	0.894
4H-3, 70-70.1	29.20	1.246
4H-5, 70-70.1	32.20	1.120
4H-7, 23-23.1	34.73	0.991
5H-1, 70-70.1	35.70	0.878
5H-3, 70-70.1	38.75	0.967
5H-5, 70-70.1	41.70	1.001
5H-7, 23.5-23.6	44.24	1.065
6H-1, 70-70.1	45.40	1.127
6H-3, 70-70.1	48.25	1.126
6H-5, 70-70.1	51.20	1.129
6H-7, 27-27.1	53.77	1.229
7H-1, 75-75.1	54.75	1.233
7H-3, 75-75.1	57.75	1.086
7H-5, 70-70.1	60.70	1.098
7H-7, 44-44.1	63.44	0.875

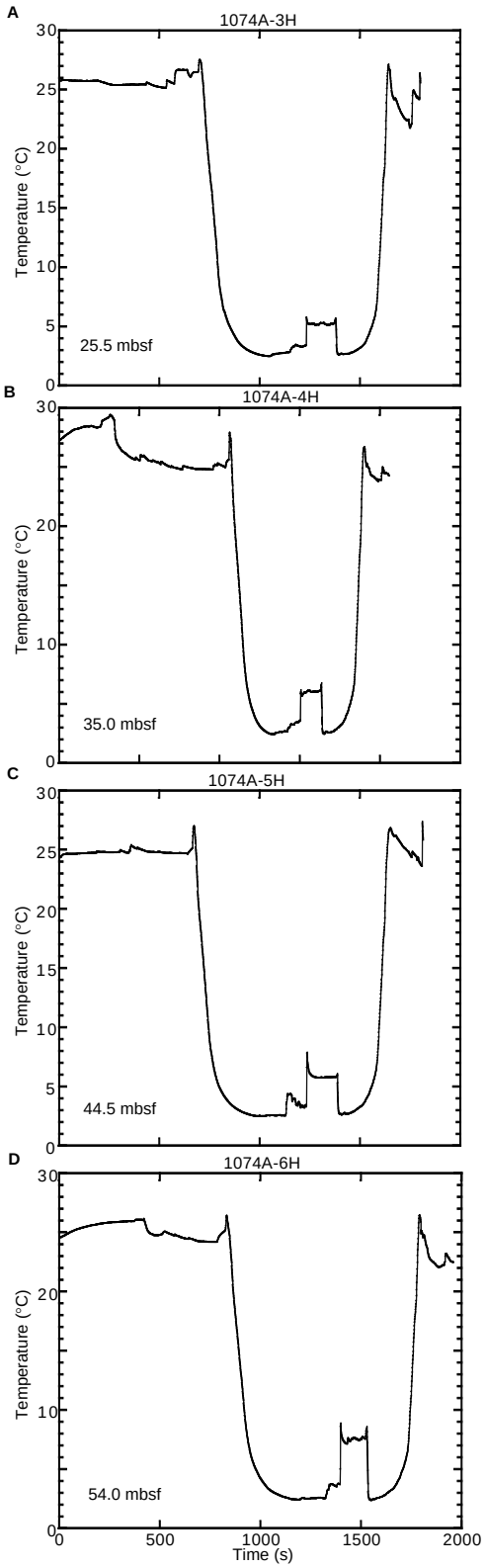

Figure 10. In situ temperature measurements for four separate deployments of the Adara core shoe temperature probe in Hole 1074A. Each plot shows temperature vs. time. The part of each curve that was analyzed is the sharp increase and then the decay that occurs over the temperature range of 3°–9°C in the center of each plot.

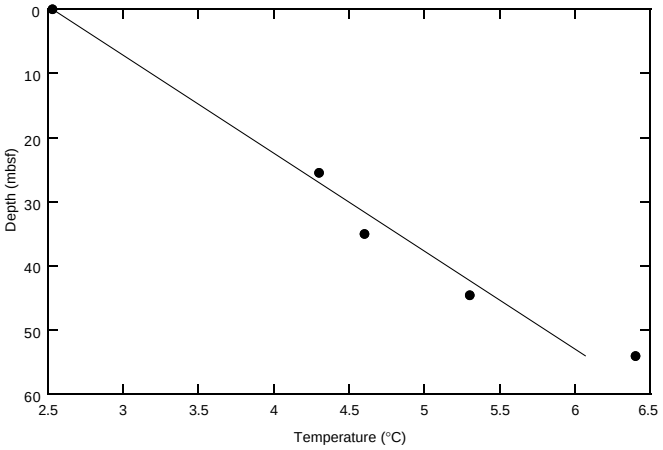

Figure 11. Interpreted in situ temperature derived from the four Adara temperature runs. A linear regression is fit to the data by forcing the line to fit the estimated bottom-water temperature (2.5°C).